A Simplified Quaternion-Based Algorithm for Orientation Estimation From Earth Gravity and Magnetic Field Measurements

Xiaoping Yun, *Fellow, IEEE*, Eric R. Bachmann, *Member, IEEE*, and Robert B. McGhee, *Life Fellow, IEEE*

***Abstract*—Orientation of a static or slow-moving rigid body can be determined from the measured gravity and local magnetic field vectors. Some formulation of the QUaternion ESTimator (QUEST) algorithm is commonly used to solve this problem. Triads of accelerometers and magnetometers are used to measure gravity and local magnetic field vectors in sensor coordinates. In the QUEST algorithm, local magnetic field measurements affect not only the estimation of yaw but also that of roll and pitch. Due to the deviations in the direction of the magnetic field vector between locations, it is not desirable to use magnetic data in calculations that are related to the determination of roll and pitch. This paper presents a geometrically intuitive 3-degree-of-freedom (3-DOF) orientation estimation algorithm with physical meaning [which is called the factored quaternion algorithm (FQA)], which restricts the use of magnetic data to the determination of the rotation about the vertical axis. The algorithm produces a quaternion output to represent the orientation. Through a derivation based on half-angle formulas and due to the use of quaternions, the computational cost of evaluating trigonometric functions is avoided. Experimental results demonstrate that the proposed algorithm has an overall accuracy that is essentially identical to that of the QUEST algorithm and is computationally more efficient. Additionally, magnetic variations cause only azimuth errors in FQA attitude estimation. A singularity avoidance method is introduced, which allows the algorithm to track through all orientations.**

***Index Terms*—Accelerometers, inertial sensors, magnetic sensors, motion measurement, orientation estimation, quaternions.**

I. Introduction

ACCURATE real-time tracking of the orientation or attitude of rigid bodies has applications in robotics, aerospace, underwater vehicles, synthetic reality, etc. For synthetic reality applications, the human body can be viewed as an articulated rigid body consisting of approximately 15 links. If the orientation relative to a fixed reference frame can be determined for each of the links, then the overall posture of the human subject can accurately be rendered and communicated in real time. The orientation of a static or slow-moving individual limb segment can be measured through the attachment of an inertial/magnetic sensor module. Such sensor modules typically contain a triad of orthogonally mounted accelerometers and a triad of orthogonally mounted magnetometers. The accelerometers are used to measure the gravity vector that is relative to the coordinate frame of the sensor module. The magnetometers serve a similar function for the local magnetic field vector. Since accelerometers actually sense the sum of gravity and linear acceleration due to motion, low-pass filtering is generally required to discriminate against the latter. In dynamic applications such as rapid human movement, a triad of angular rate sensors is usually added as a "complementary" high-frequency source of orientation information. In any case, such approaches to orientation estimation are dependent only on passive measurement of physical quantities that are directly related to the rate of rotation and orientation of a rigid body. Since no generated signals are involved, there are no restrictions on the range of operation. All latency in such a system is due to the computational demands of the data processing algorithms and not due to the physical characteristics of a generated source.

Extensive research has been conducted to investigate full 3-degree-of-freedom (3-DOF) orientation tracking using inertial/magnetic sensor modules. Foxlin *et al.* [1], [2] describe two commercial nine-axis sensing systems designed for head-tracking applications. Bachman *et al.* proposed a quaternion-based complementary filter for human-body-motion tracking. The filter is able to track through all orientations without singularities and continuously correct for drift without a need for stationary periods using nine-axis inertial/magnetic sensor module data [3], [4]. Gallagher *et al.* presents a simpler complementary filter algorithm with lower computational complexity in [5]. Luinge describes a Kalman filter that is designed for human-body-tracking applications. The filter is based on the use of accelerometers and rate sensors. The drift about the vertical axis is reduced by limiting body segment orientation using a kinematic human body model [6]. Rather than estimating individual limb segment orientations relative to a fixed reference frame, Zhu and Zhou [7] determine joint angles in axis/angle form using the data from the two nine-axis sensors that are mounted on the inboard and outboard sides of the joint. Yan and Yuan [8] describe an orientation-tracking algorithm that uses low-cost sensor modules to take two-axes measurements of gravity and the local magnetic field. In a manner that is similar to the method described in this paper, elevation, roll, and azimuth angles are sequentially calculated. The angles are used to construct rotation matrices, and the use of trigonometric functions is required. The method is limited to orientation tracking within a hemisphere. In [9], Gebre-Egziabher *et al.* describe an attitude-determination

Manuscript received July 9, 2006; revised October 12, 2007. This work was supported in part by the U.S. Army Research Office.

X. Yun is with the Department of Electrical and Computer Engineering, Naval Postgraduate School, Monterey, CA 93943 USA.

E. R. Bachmann is with the Department of Computer Science and System Analysis, Miami University, Oxford, OH 45056 USA.

R. B. McGhee is with the Department of Computer Science and MOVES Institute, Naval Postgraduate School, Monterey, CA 93943 USA.

Digital Object Identifier 10.1109/TIM.2007.911646

algorithm for aircraft applications. The algorithm is based on a quaternion formulation of Wahba's problem [10], where magnetometer and accelerometer measurements are used to determine attitude.

The TRIAD algorithm [11] is a single frame deterministic method for solving Wahba's problem. It requires normalized measurements of two nonparallel reference vectors as input. It produces a suboptimal orientation estimate in the form of a 3×3 rotation matrix. The algorithm constructs two triads of orthonomal unit vectors. The two triads are the components of an inertial frame expressed in both the body and Earth-fixed reference frames. Let ${}^{b}a$ and ${}^{b}m$ be the normalized accelerometer and magnetometer measurements that are relative to the body frame of the gravity and magnetic field reference vectors (${}^{E}g$ and ${}^{E}m$). The reference vectors are expressed relative to an Earth-fixed frame, and like the measurement vectors, they are normalized to unit length. The first triad is given by

$$\hat{s}_1 = {}^{E}g \tag{1}$$

$$\hat{s}_2 = \frac{({}^{E}g \times^{E} m)}{|{}^{E}g \times^{E} m|} \tag{2}$$

$$\hat{s}_3 = \hat{s}_1 \times \hat{s}_2. \tag{3}$$

The second triad is given by

$$\hat{r}_1 = {}^{b}a \tag{4}$$

$$\hat{r}_2 = \frac{({}^{b}a \times^{b} m)}{|{}^{b}a \times^{b} m|} \tag{5}$$

$$\hat{r}_3 = \hat{r}_1 \times \hat{r}_2. \tag{6}$$

These triads are then used to create measurement and reference matrices

$$M_{\text{mea}} = [\hat{r}_1\ \hat{r}_2\ \hat{r}_3], \quad M_{\text{ref}} = [\hat{s}_1\ \hat{s}_2\ \hat{s}_3]. \tag{7}$$

The orientation matrix A representing the attitude of a rigid body is then simply

$$A = M_{\text{mea}}\, M_{\text{ref}}^{T}. \tag{8}$$

If the measurements of the gravity and the magnetic field are ordered as described earlier, the cross-products that are used to calculate $\hat{s}_2$ and $\hat{r}_2$ eliminate any contribution of the magnetic measurements relative to the vertical axis. Thus, pitch and roll components of orientation are determined using only the accelerometer measurements.

The QUaternion ESTimator (QUEST) algorithm is a popular algorithm for single-frame estimation of a quaternion that represents the attitude of a rigid body relative to a fixed coordinate system. The algorithm was created to solve Wahba's problem [10] in the context of spacecraft attitude determination. Given a set of 3-D known reference unit vectors $V_1, V_2, \ldots, V_n$ and a set of the corresponding observation or measurement unit vectors $W_1, W_2, \ldots, W_n$ (which could be the direction of the sun or a star observed from a spacecraft measured in the spacecraft's body frame), Wahba's problem is to find the least squares estimate of spacecraft attitude by minimizing the following loss function:

$$L(A) = \frac{1}{2}\sum_{i=1}^{n} a_i (W_i - AV_i)^T (W_i - AV_i) \tag{9}$$

with respect to the 3×3 orthogonal orientation matrix A, where $a_1, a_2, \ldots, a_n$ are nonnegative weighting coefficients. The minimum number of measurement and reference vector pairs is two. Early solutions to Wahba's problem directly computed the orientation matrix A [12]. Davenport [13] introduced a method of parameterizing the orientation matrix by a unit quaternion q and proved that the loss function (9) can be transformed into a quadratic gain function of the unit quaternion in the form of

$$G\left(A(q)\right) = \sum_{i=1}^{n} a_i - L\left(A(q)\right) = q^T K q \tag{10}$$

where K is a 4×4 matrix constructed from the reference vectors V_i, measurement vectors W_i, and weighting coefficients a_i, $i = 1, 2, \ldots, n$. Based on Davenport's work, Shuster and Oh derived the QUEST algorithm [14] and showed that the optimal quaternion q that maximizes the gain function (10) while satisfying the unit quaternion (unit norm) constraint is the eigenvector of the K matrix corresponding to the largest eigenvalue of K. Thus, the problem is reduced to finding the eigenvalues and eigenvectors of a 4×4 matrix.

In body-tracking applications based on the use of small inertial/magnetic sensors [4], the gravity and local magnetic field vectors are often measured and compared to reference vectors in order to determine orientation. In the case of the gravity vector, the assumption that it is fixed leads to no difficulties since this vector points straight down in any inertial frame located on or near the surface of the Earth. Making the same assumption regarding the local magnetic field vector can lead to problems. In a typical room setting, the direction of the local magnetic field vector can be expected to vary due to the presence of ferrous objects or electrical appliances. In inertial/magnetic-tracking algorithms, the local magnetic field vector is commonly treated as a fixed reference. It is assumed that this reference will remain constant. If it does not, algorithms such as QUEST will be prone to errors not only in azimuth but also in pitch and roll.

This paper presents an alternative algorithm for estimating orientation based on a set of measurements from triads of orthogonally mounted magnetometers and accelerometers. It is called the *factored quaternion algorithm* (FQA). It is an intuitive alternative to the TRIAD and QUEST algorithms that yields certain advantages. In the FQA, local magnetic field data are used only in azimuth angle calculations. This decoupling of accelerometer and magnetometer data eliminates the influence of magnetic variations on calculations that determine pitch and roll. Through a derivation based on half-angle formulas, the computational cost of computing trigonometric functions is avoided. The algorithm produces a quaternion output. It is able to track through all orientations without singularities. The FQA and the TRIAD algorithm produce an equivalent solution to the same problem, with the exception that the former

produces a quaternion, and the latter produces a rotation matrix. Experimental results in which the FQA is compared with the QUEST algorithm indicate that it has nearly identical accuracy at a comparable or lower computational expense. The QUEST algorithm was chosen as a benchmark for comparison because it is an optimal algorithm and produces orientation estimates in quaternion form, as does the FQA.

The primary contributions of this paper are the following:

1) derivation of a new geometrically intuitive algorithm for determining orientation that is relative to an Earth-fixed reference frame based on a set of accelerometer and magnetometer measurements;
2) a singularity avoidance method that allows the algorithm to track through all orientations;
3) experimental results which validate the performance of the algorithm.

The rest of this paper is organized as follows. Section II presents the derivation of the FQA. Section III describes the experiments in which the factored algorithm is compared to the QUEST algorithm for efficiency and accuracy. The ability of the algorithm to track through all orientations without singularities is demonstrated as is its decoupling property. The final section discusses the experimental results and provides a summary.

II. Factored Quaternion Algorithm (FQA)

The FQA presented in this section is for estimating the orientation of a static or slow-moving rigid body based on Earth gravity and magnetic field measurements [15]. This algorithm is not applicable to situations in which relatively large linear accelerations due to dynamic motion are present, unless it is used in a complementary or optimal filter together with angular rate information. Sensor modules such as MARG III, which is described in [16], contain a triad of accelerometers, a triad of magnetometers, and a triad of angular rate sensors, and it can be used to provide measurement data for the FQA.

In a typical application, a sensor module is employed as a strap down inertial measurement unit (IMU) that is attached to a rigid body whose orientation is to be determined. To facilitate the analysis, it is convenient to define three coordinate systems. An Earth-fixed coordinate system $x_e y_e z_e$ is defined to follow the North–East–down (NED) convention, i.e., x_e points North, y_e points East, and z_e points down. A body coordinate system $x_b y_b z_b$ is attached to the rigid body whose orientation is to be measured. The sensor module has its own coordinate system $x_s y_s z_s$ corresponding to the axes of three orthogonally mounted accelerometers/magnetometers. Since the sensor module is rigidly attached to the rigid body, the body coordinate system $x_b y_b z_b$ differs from the sensor coordinate system $x_s y_s z_s$ by a constant offset. For the convenience of discussions, in what follows, the body coordinate system is assumed to coincide with the sensor coordinate system.

A. Quaternion Rotation Operator

According to Euler's theorem on finite rotations, an arbitrary sequence of rotations in space can always be described by a rotation about a certain axis through a specified angle. Let

$$u = \begin{bmatrix} u_1 \\ u_2 \\ u_3 \end{bmatrix} \tag{11}$$

be the unit vector in 3-D space that represents the rotation axis, and let β be the rotation angle. The Euler parameters are defined by

$$q_0 = \cos\left(\frac{\beta}{2}\right) \tag{12}$$

$$\begin{bmatrix} q_1 \\ q_2 \\ q_3 \end{bmatrix} = u \sin\left(\frac{\beta}{2}\right) = \begin{bmatrix} u_1 \\ u_2 \\ u_3 \end{bmatrix} \sin\left(\frac{\beta}{2}\right). \tag{13}$$

Because an arbitrary rotation may be described by three independent parameters, the four Euler parameters are constrained to satisfy the relation [17]

$$q_0^2 + q_1^2 + q_2^2 + q_3^2 = 1. \tag{14}$$

These four parameters are also referred to as a *unit quaternion*, which is commonly written in the form

$$q = (q_0\ q_1\ q_2\ q_3) \tag{15}$$

where q_0 is the scalar (or real) part, and $[q_1\ q_2\ q_3]^T$ is the vector part. Unit quaternions can be used to perform rotation operations in 3-D space [18]. Specifically, for any vector $v = [v_1\ v_2\ v_3]^T$ in 3-D space, the following operation produces a vector v' by rotating the vector v about the axis that is defined by u through an angle β:

$$v' = qvq^{-1} \tag{16}$$

In this expression, all multiplications are quaternion multiplications, v and v' are treated as pure vector quaternions whose real part is zero, and q^{-1} is the *inverse* quaternion of q [18].

B. Elevation Quaternion

A rigid body is said to be in its *reference orientation* when its $x_b y_b z_b$-axes are aligned with those of the Earth coordinate system. It is known that a rigid body can be placed in an arbitrary orientation by first rotating it about its z-axis by an angle ψ (azimuth or yaw rotation), then about its y-axis by angle θ (elevation or pitch rotation), and finally about its x-axis by angle ϕ (bank or roll rotation).

In order to derive a quaternion describing only elevation, it is useful to note that, when a rigid body is moving at a constant velocity and is in a fixed orientation, an accelerometer measures only gravity. Furthermore, the x-axis accelerometer senses only the component of gravity along the x-axis, and this component, in turn, depends only on the elevation angle. This can be seen from the following argument. Starting with the rigid body in its reference orientation, the x-axis accelerometer is perpendicular

to gravity and thus registers zero acceleration. The y-axis accelerometer also reads zero, while the z-axis accelerometer reads $-g$. If the body is then rotated in azimuth about its z-axis, the x-axis accelerometer still reads zero, regardless of the azimuth angle. If the rigid body is next pitched up through an angle θ, the x-axis accelerometer will read

$$a_x = g \sin\theta \tag{17}$$

and the z-axis accelerometer will read

$$a_z = -g \cos\theta \tag{18}$$

where $g = 9.81$ m/s^2 is the gravitational acceleration, and

$$a = \begin{bmatrix} a_x \\ a_y \\ a_z \end{bmatrix} \tag{19}$$

is the measured acceleration vector in the body coordinate system. For convenience, the accelerometer and magnetometer outputs from a sensor module are normalized to unit vectors. Let $\bar{a}$ denote the *normalized* vector of the acceleration measurements

$$\bar{a} = \frac{a}{|a|} = \begin{bmatrix} \bar{a}_x \\ \bar{a}_y \\ \bar{a}_z \end{bmatrix} \tag{20}$$

where $|a|$ is the norm of the acceleration vector a. It follows from (17) that the value for $\sin\theta$ can be expressed as

$$\sin\theta = \bar{a}_x. \tag{21}$$

The value for $\cos\theta$ can be computed from

$$\cos\theta = \sqrt{1 - \sin^2\theta}. \tag{22}$$

It should be noted that a positive value for $\cos\theta$ is assumed in the preceding equation. This is because the elevation angle θ is, by convention, restricted to the range of $-\pi/2 \le \theta \le \pi/2$, and $\cos\theta$ is positive over this entire range. In addition, if the rigid body is rolled about its x-axis, (18) will change, but (17) will remain the same. This means that (17) holds for any orientation of the rigid body.

In order to obtain an elevation quaternion using (12) and (13), a value is needed for $\sin(\theta/2)$ and $\cos(\theta/2)$. From trigonometric half-angle formulas, half-angle values are given by

$$\sin\frac{\theta}{2} = \text{sign}(\sin\theta)\sqrt{(1-\cos\theta)/2} \tag{23}$$

$$\cos\frac{\theta}{2} = \sqrt{(1+\cos\theta)/2} \tag{24}$$

where $\text{sign}()$ is the sign function that returns $+1$ for positive arguments and -1 for negative arguments. The sign function is not needed in (24) since $\cos(\theta/2)$ is always positive within the elevation angle range.

Elevation is a rotation about the y-axis. The unit quaternion representing elevation can now be computed using (12) and (13), and values for the half-angle trigonometric functions are as follows:

$$q_e = \cos\frac{\theta}{2}(1\ 0\ 0\ 0) + \sin\frac{\theta}{2}(0\ 0\ 1\ 0). \tag{25}$$

C. Roll Quaternion

The acceleration measured by the z-axis accelerometer with roll angle $\phi = 0$ is given by (18). Changing the azimuth angle does not alter this measurement, but changing roll does. A more general formula for y-axis accelerometer reading is

$$a_y = -g \cos\theta \sin\phi. \tag{26}$$

Likewise, the z-axis accelerometer will read

$$a_z = -g \cos\theta \cos\phi. \tag{27}$$

In terms of the normalized acceleration measurement, the earlier two equations can be written as

$$\bar{a}_y = -\cos\theta \sin\phi \tag{28}$$

$$\bar{a}_z = -\cos\theta \cos\phi \tag{29}$$

where the value for $\cos\theta$ is determined by (22). If $\cos\theta$ is not equal to zero, the values of $\sin\phi$ and $\cos\phi$ can easily be determined by

$$\sin\phi = -\bar{a}_y/\cos\theta \tag{30}$$

$$\cos\phi = -\bar{a}_z/\cos\theta. \tag{31}$$

If $\cos\theta$ is equal to zero, it means that x-axis of the body coordinates is vertically oriented. In such cases, the roll angle is undefined, and it can be assumed to have a value that is equal to zero. The range of the roll angle ϕ is by convention restricted to $-\pi < \phi \le \pi$. Thus, the half-angle values for ϕ can be computed in a manner that is similar to (23) and (24), with one exception. When $\cos\phi = -1$ and $\sin\phi = 0$, the use of (23) and (24) will result in a value of zero for both $\sin(\phi/2)$ and $\cos(\phi/2)$. This case can be treated in implementation by assigning a value of one to the sign function when its argument is zero. Having obtained the half-angle sine and cosine values for the roll angle ϕ, the roll quaternion is computed as follows:

$$q_r = \cos\frac{\phi}{2}(1\ 0\ 0\ 0) + \sin\frac{\phi}{2}(0\ 1\ 0\ 0). \tag{32}$$

D. Azimuth Quaternion

Since azimuth rotation has no effect on the estimation of roll or elevation quaternions from the accelerometer data, the strategy employed in this paper for azimuth quaternion estimation is to first solve for the elevation and roll quaternions.

These can then be used to rotate the normalized magnetic field measurement vector in the body coordinate system

$$ {}^{b}m = \begin{bmatrix} {}^{b}m_x \\ {}^{b}m_y \\ {}^{b}m_z \end{bmatrix} \tag{33} $$

into an intermediate Earth coordinate system by the quaternion rotation operation

$$ {}^{e}m = q_e \; q_r \; {}^{b}m \; q_r^{-1} \; q_e^{-1}. \tag{34} $$

In this expression, ${}^{b}m$ stands for the pure vector quaternion of the 3-D vector itself, i.e., ${}^{b}m = (0 \; {}^{b}m_x \; {}^{b}m_y \; {}^{b}m_z)$. The same convention is used for ${}^{e}m$. In the absence of measurement error, ${}^{e}m$ should agree with the known local normalized magnetic field vector $n = [n_x \; n_y \; n_z]^T$, except for the effects of azimuth rotation on the sensor magnetometer readings. In such a case, $n_z = {}^{e}m_z$, and

$$ \begin{bmatrix} n_x \\ n_y \end{bmatrix} = \begin{bmatrix} \cos\psi & -\sin\psi \\ \sin\psi & \cos\psi \end{bmatrix} \begin{bmatrix} {}^{e}m_x \\ {}^{e}m_y \end{bmatrix} \tag{35} $$

where ψ is the azimuth angle. Before proceeding further, it should be noted that (35) implies that the two 2-D vectors differ only in orientation. In fact, the experimental data show that, in the presence of magnetic interference and measurement noise, they may also differ in length. To compensate for this effect, the vectors on both sides of (35) can be normalized. Specifically, let the normalized local magnetic field reference vector in the horizontal plane be

$$ N = \begin{bmatrix} N_x \\ N_y \end{bmatrix} = \frac{1}{\sqrt{n_x^2 + n_y^2}} \begin{bmatrix} n_x \\ n_y \end{bmatrix} \tag{36} $$

and the corresponding quantity measured by the magnetometer be

$$ M = \begin{bmatrix} M_x \\ M_y \end{bmatrix} = \frac{1}{\sqrt{{}^{e}m_x^2 + {}^{e}m_y^2}} \begin{bmatrix} {}^{e}m_x \\ {}^{e}m_y \end{bmatrix}. \tag{37} $$

With these definitions, (35) becomes

$$ \begin{bmatrix} N_x \\ N_y \end{bmatrix} = \begin{bmatrix} \cos\psi & -\sin\psi \\ \sin\psi & \cos\psi \end{bmatrix} \begin{bmatrix} M_x \\ M_y \end{bmatrix} \tag{38} $$

from which the value of $\cos\psi$ and $\sin\psi$ can be solved as

$$ \begin{bmatrix} \cos\psi \\ \sin\psi \end{bmatrix} = \begin{bmatrix} M_x & M_y \\ -M_y & M_x \end{bmatrix} \begin{bmatrix} N_x \\ N_y \end{bmatrix}. \tag{39} $$

The azimuth angle ψ is restricted to the range $-\pi < \psi \leq \pi$. The half-angle formulas given by (23) and (24) can again be used to compute the half-angle sine and cosine values for ψ. The azimuth quaternion is then given by

$$ q_a = \cos\frac{\psi}{2}(1\;0\;0\;0) + \sin\frac{\psi}{2}(0\;0\;0\;1). \tag{40} $$

Having obtained all three rotation quaternions, the quaternion estimate representing the orientation of the rigid body is finally given by

$$ \hat{q} = q_a \; q_e \; q_r. \tag{41} $$

E. Singularity Avoidance in Implementation

The FQA presented earlier takes the normalized acceleration measurement vector and the normalized local magnetic field measurement vector as its inputs, and it produces a quaternion, which is its output. It is a single-frame algorithm, i.e., it takes measurements at a single instant of time and produces an output. It does not require a history of measurements at multiple instants of time.

From the two measurement vectors, the half-angle values of sine and cosine for each rotation angle are first computed. Then, the corresponding quaternion for each rotation is computed. Finally, the overall orientation quaternion is computed by (41). It should be emphasized that the algorithm does not evaluate trigonometic functions at any step.

Although quaternions, when used to represent the 3-D orientation, do not have singularities, the FQA described earlier uses three angles to derive the quaternion estimate. It is known that any three-parameter representation of 3-D orientation is inevitably singular at some point [19]. Without exception, the FQA has a singularity, as does the QUEST algorithm. The QUEST algorithm uses the Gibbs vector

$$ \rho = \frac{1}{q_0} \begin{bmatrix} q_1 \\ q_2 \\ q_3 \end{bmatrix} \tag{42} $$

in its derivation and is at a singular point if $q_0 = 0$. A method that is similar to the method of sequential rotations discussed in [20] is described below to avoid singularities in the numerical implementation. A singularity occurs in the FQA if the elevation angle is $\pm 90^\circ$. This happens when $\cos\theta = 0$ in (30) and (31). In implementation, the first step of the algorithm is to check the value of $\cos\theta$. If the value of $\cos\theta$ is smaller than a predefined constant ϵ (e.g., $\epsilon = 0.1$), the procedures described below are implemented to circumvent the numeric difficulty of having a small number in the denominator.

If $\cos\theta \leq \epsilon$, the elevation angle is close to $\pm 90^\circ$. To deal with this situation, the normalized acceleration measurement vector $\bar{a}$ and normalized magnetic field measurement vector ${}^{b}m$ in the body frame are rotated about the body coordinate y_b-axis by an angle α to obtain the following offset (rotated) measurement vectors:

$$ \bar{a}_{\text{offset}} = q_\alpha \; \bar{a} \; q_\alpha^{-1} \tag{43} $$

$$ {}^{b}m_{\text{offset}} = q_\alpha \; {}^{b}m \; q_\alpha^{-1} \tag{44} $$

where q_α is the offset (rotation) quaternion given by

$$ q_\alpha = \cos\frac{\alpha}{2}(1\;0\;0\;0) + \sin\frac{\alpha}{2}(0\;0\;1\;0). \tag{45} $$

Under the condition of $\cos\theta \leq \epsilon$, the offset measurement vectors will be used in place of the original measurement vectors to carry out the FQA. The resultant orientation quaternion estimate from (41), in this case, is called $\hat{q}_{\text{alt}}$.

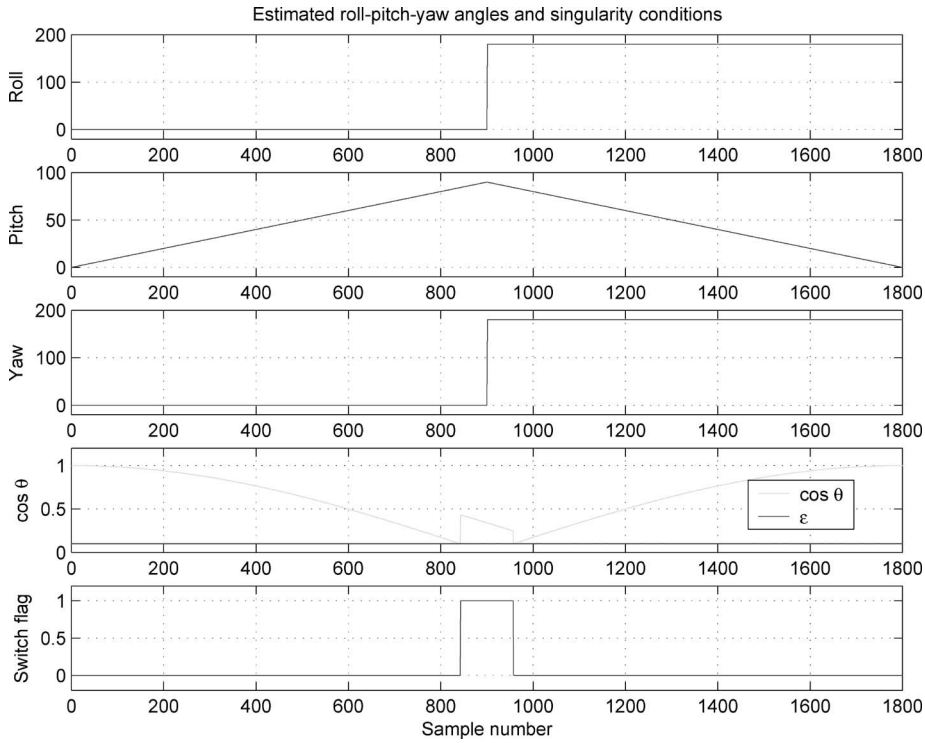

Fig. 1. Roll, pitch, and yaw angles; singularity condition; and switch flag during a 180° rotation about the pitch axis with ideal simulated data.

The value of α can arbitrarily be chosen as long as it is sufficiently far away from zero. It is chosen to be 20° in this discussion. Rotating measurement vectors about y_b-axis by 20° is equivalent to rotating the (original) body coordinate system $x_b y_b z_b$ to a temporarily offset body coordinate system $x_b' y_b' z_b'$ about the y_b-axis by $-20°$. The symbol $\hat{q}_{\rm alt}$ represents the orientation of $x_b' y_b' z_b'$ in the Earth coordinate system. The quaternion estimate $\hat{q}$ representing the orientation of the original body coordinate system $x_b y_b z_b$ is given by the following compound quaternion (i.e., rotating $x_b' y_b' z_b'$ back to $x_b y_b z_b$ about the y_b'-axis by 20°):

$$\hat{q} = \hat{q}_{\rm alt}\ q_\alpha. \tag{46}$$

To demonstrate how the singularity avoidance method works, ideal measurements as well as noisy measurements for a 180° rotation about the pitch axis were synthetically generated. Fig. 1 shows the results with ideal measurements. The top three plots are trajectories of roll, pitch, and yaw angles. The bottom two plots depict the value of $\cos\theta$ and the switch flag. The value of $\cos\theta$ is an indication of the singularity condition, and the switch flag indicates when the singularity avoidance method is invoked. As expected, the pitch angle increases from 0° to 90°, while the roll and yaw angles remain at zero during the first half period. As the pitch angle approaches 90°, the value of $\cos\theta$ drops nearly to zero. When $\cos\theta$ is less than ϵ (whose value is chosen as 0.1 in this testing), the singularity avoidance method is activated during the period of sample numbers from about 820 to 980, as shown in Fig. 1. During this period, the value of $\cos\theta$ is lifted upwards to be away from zero. The value of the offset angle α is chosen to be 20°.

Owing to the conventional choice, the pitch angle is limited from $-90°$ to 90°. As a result, the orientation of 95° pitch, 0° roll, and 0° yaw is depicted as 85° pitch, 180° roll, and 180° yaw in Fig. 1. This is the reason why the pitch angle increases from 0° to 90° and then decreases from 90° to 0°, while in the actual rotation, it increases from 0° to 180°.

Fig. 2 shows the results with noisy measurements for the same rotational motion as in Fig. 1. Noise signals were introduced using a random number generator. It is noted that the switch flag flipped many times, and the value of $\cos\theta$ was kept above $\epsilon = 0.1$ at all times. The trajectory of the pitch angle follows the same rise and fall pattern as in Fig. 1, except with added noise. The roll and yaw angles flipped from 0° to 180° numerous times, signifying that the pitch angle jumped above and below 90°. Figs. 1 and 2 show the trajectory of the roll, pitch, and yaw angles for visualization purposes. Although there are jumps in roll and yaw, there are no jumps in the trajectory of the estimated quaternion, as shown in the corresponding plot of the estimated quaternion components in Fig. 3.

F. Alternative Method for Singularity Avoidance

The aforementioned procedure amounts to a second (virtual) sensor package that is offset from the basic (physical) sensor package by a rotation of $-20°$ about the body right-side coordinate axis (y_b-axis). In this method, when the physical sensor approaches an Euler angle singularity (as indicated by the switch flag), the virtual sensor data are substituted for the physical sensor data, thereby avoiding division by a small number and attendant sensitivity to noise in calculating the desired orientation quaternion. An alternative to this approach is to use a second set of Euler angles such that the second set has its singularities located in a different spatial orientation than the ϕ, θ, and ψ *aerospace* sets [18] that are used so far in

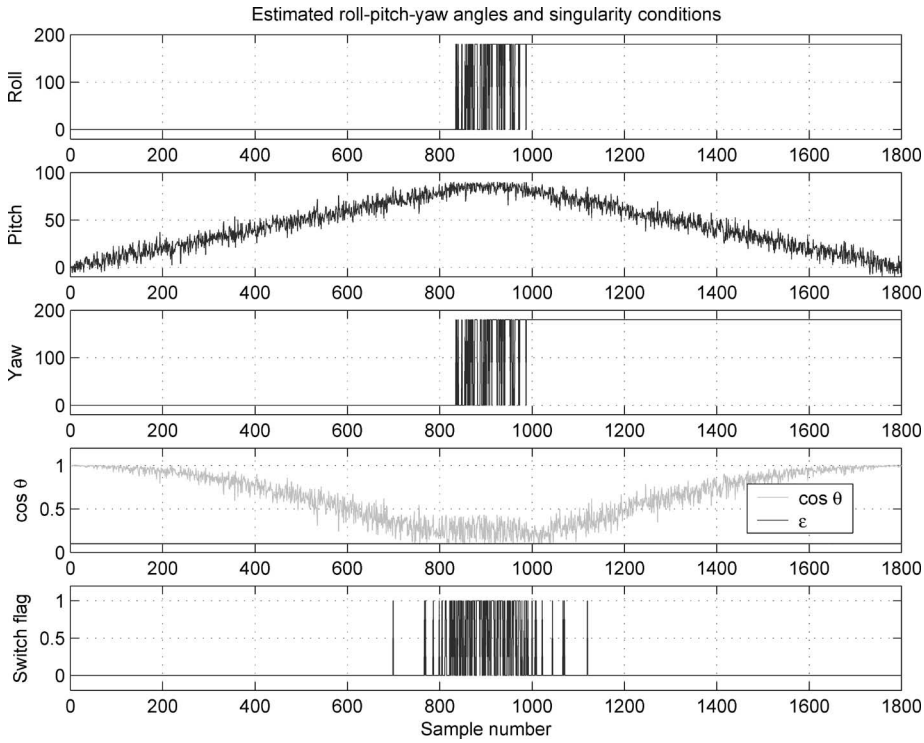

Fig. 2. Roll, pitch, and yaw angles; singularity condition; and switch flag during a 180° rotation in pitch axis with noisy simulated data. The parameters used are $\epsilon = 0.1$ and the offset angle $\alpha = 20°$.

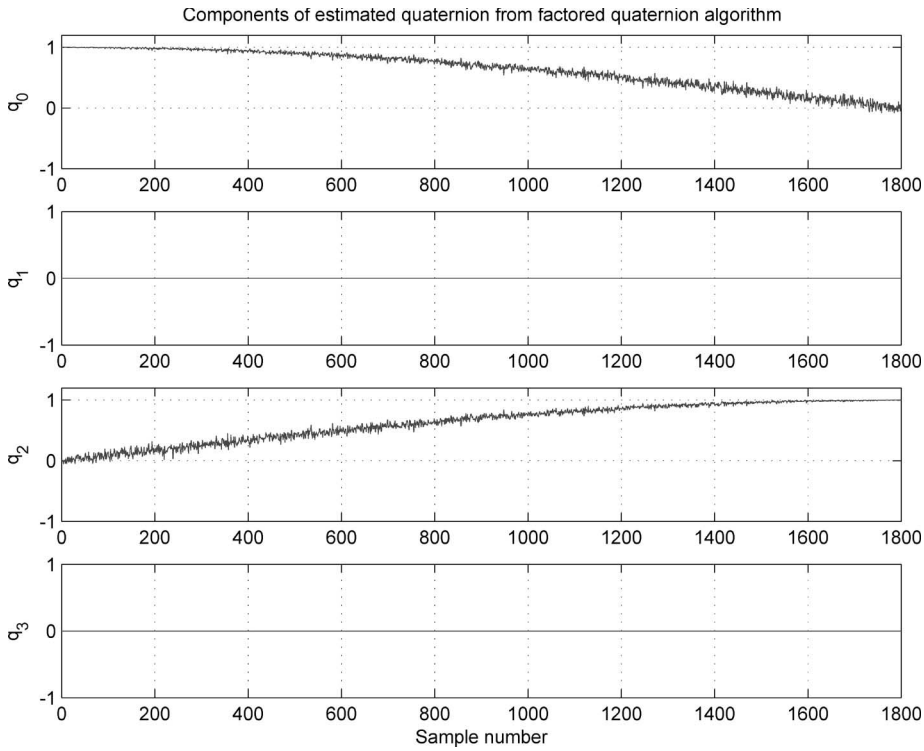

Fig. 3. Components of the estimated quaternion during a 180° rotation about the pitch axis with noisy simulated data.

this paper and to switch between these sets as needed to avoid singularities. This possibility is explored in the following discussion.

Per earlier discussion, one interpretation of the aerospace Euler angles [18] is that, starting with body axes (nose, right side, and belly) aligned with Earth axes (North, East, and down), ψ is the *yaw* angle associated with rotation of an object about its belly axis. This is followed by a *pitch* rotation θ about the (rotated) right-side axis and, finally, a *roll* rotation ϕ about the (rotated) nose axis. It should be noted that the aforementioned reserved names for these angles are alternatively referred to, respectively, as *azimuth*, *elevation*, and *bank* angles [18].

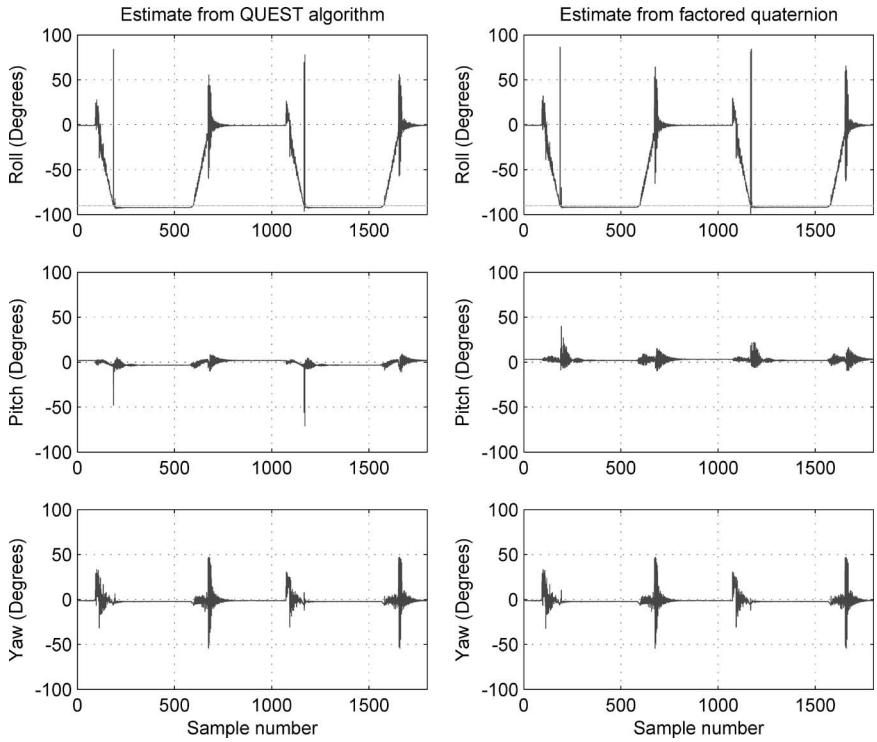

Fig. 4. Orientation estimate produced by the QUEST algorithm and FQA with a periodic 90° rotation about the roll axis using accelerometer and magnetometer data.

The former names are frequently used when thinking about rotations viewed from the object (for example, as by a pilot), while the latter names are more commonly used by observers situated in an Earth-fixed coordinate system (for example, as in field artillery).

An instance of an alternate set of Euler angles is provided by the angles resulting from exchanging the temporal order of the first two rotations described earlier. If this is done, due to the well-known noncommutativity of finite rotations, the resulting angles will have different values as compared to the aerospace set. Furthermore, the singularities of the alternate set will occur in a different orientation. To see that this is so, consider an object initially aligned in the reference orientation described earlier. If this object is subjected first to a 90° rotation about its right-side axis (y_b-axis), its belly axis (z_b-axis) will then point North. A subsequent rotation of 90° about this (rotated) belly axis will cause the nose axis of the object to point East, corresponding to the axis of the first rotation. Further reflection on this analysis shows that, for *any* initial right-side (East) axis rotation, if this is followed by a $\pm 90^\circ$ belly axis rotation, the object nose axis will point either East or West; in either case, it will be parallel to the initial rotation axis. These are, by definition, *singular* conditions, which are sometimes called the *gimbal lock*. On the other hand, from (30) and (31), for the standard aerospace Euler angles, singularities exist if and only if the object nose axis points straight up or down. This means that singularities in the formulas used for determination of the orientation quaternion can be avoided by switching between these two Euler angle sets as needed.

Evidently, the use of alternative Euler angles requires the derivation of new formulas for the computation of the corresponding orientation quaternions as well as expressions for switching from one Euler set to the other when a singular condition is approached. While this is straightforward and certainly practical, it is believed that the use of an offset virtual sensor, as in the implementation in this paper, is both conceptually and mathematically simpler and leads to simpler computer software. Therefore, all of the following experimental results were obtained using the virtual offset sensor switching approach.

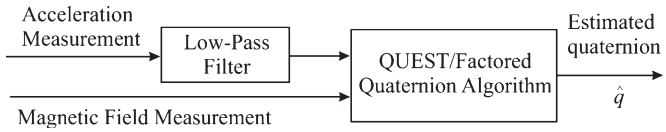

Fig. 5. Block diagram of the QUEST algorithm/FQA with a low-pass filter.

III. Experimental Results

Sensor data for the experiments were collected using a MARG III inertial/magnetic sensor module, which was designed by the authors and fabricated by McKinney Technology [16]. Primary sensing components for this unit include a pair of two-axes Analog Devices ADXL202E micromachined accelerometers, and Honeywell HMC1051Z and HMC1052 one- and two-axes magnetometers. Overall, dimensions of the MARG III unit are approximately 0.7 in $\times 1.2$ in $\times 1.0$ in. Although the MARG III units contain angular rate sensors, no rate data were used in the experiments described in this paper.

A. Testing of Static and Dynamic Accuracy

Controlled rotations of the sensor modules were performed by placing an inertial/magnetic sensor module on a HAAS

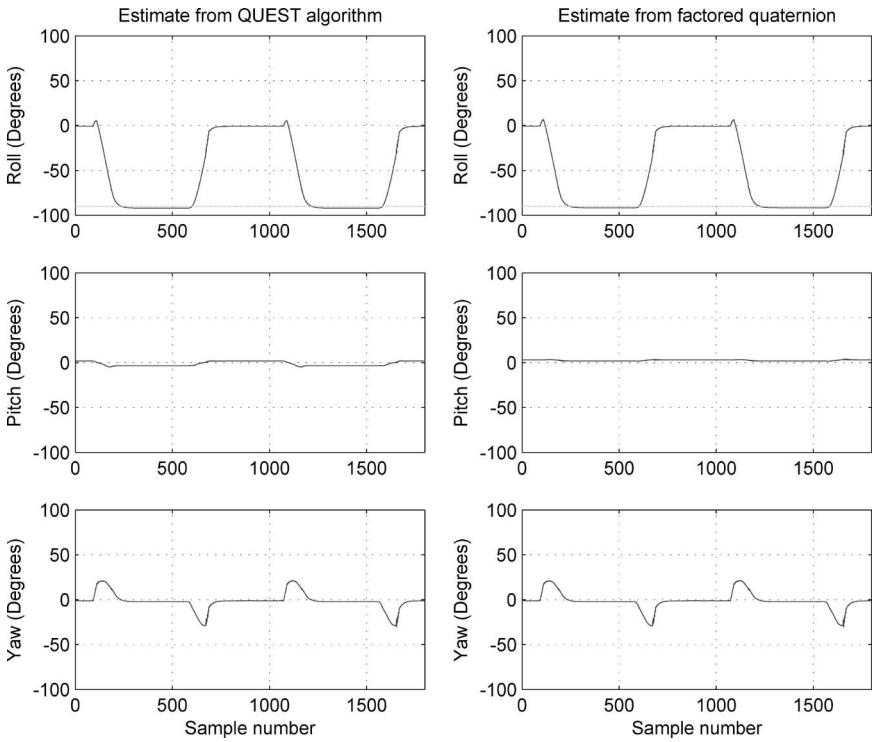

Fig. 6. Orientation estimate produced by the QUEST algorithm and FQA with a 90° rotation in roll axis using low-pass filtered accelerometer data.

precision tilt table. The table has two degrees of freedom and is capable of positioning with an accuracy of 0.001° at rates ranging from 0.001 to $80^\circ/\mathrm{s}$. In order to mitigate any possible magnetic effects generated by the steel construction of the tilt table, the sensor unit was mounted on a nonferrous extension above the table. In each of these experiments, the sensor module was initially placed with its $x_s y_s z_s$-axes, respectively, aligned with the NED directions. Following an initial still period, the sensor module was then subjected to a series of rotations.

Fig. 4 shows the performance of each of the two algorithms using raw accelerometer and magnetometer data. The sensor was rotated -90° about the x-axis at a rate of $60^\circ/\mathrm{s}$ and then rotated 90° at the same rate (in the reverse direction) for two cycles. The plots to the left show the orientation estimated by the QUEST algorithm, and the graphs to the right show the orientation estimated by the FQA. The small pitch and yaw motions seen in the pitch and yaw subplots are due to misalignment of the sensor module with the motion axes of the tilt table. It can be seen that both algorithms were able to correctly estimate the roll angle before the first (negative) rotation, between the first and second (positive) rotations, and after the second rotation. Neither was able to correctly estimate orientation during rotational motion. Similar results were observed in experiments involving different angles of rotation at different rates.

During motion, the accelerometers measure the sum of gravity and motion-induced acceleration. In the case of the experiments described here, the motion-induced acceleration is due to the motion of the tilt table and flexing of the nonferrous extension on which the sensor module was mounted. Since both the QUEST algorithm and FQA are single-frame algorithms, neither is able to filter out transient nongravitational accelerations that occur during motion.

Fig. 5 shows a revised approach in which a low-pass filter for accelerometer data is combined with the FQA or QUEST algorithm. To examine the performance of the QUEST algorithm and FQA in conjunction with a low-pass filter, the rotation experiments were repeated. Fig. 6 shows the performance during 90° rolls at a rate of $60^\circ/\mathrm{s}$. A comparison of Fig. 6 with Fig. 4, in which the sensor module was subjected to the same rotations, shows that either algorithm can be used to track the orientation of a rigid body in a dynamic environment when acceleration data are low-pass filtered. Again, similar results were observed in experiments involving different angles of rotation at different rates.

B. Avoidance of Singularity Conditions

Within the FQA, three half-angles are used to derive an orientation quaternion. Measurement vectors are rotated by an angle α when the pitch angle approaches $\pm 90^\circ$ and $\cos\theta$ approaches zero. Figs. 7 and 8, respectively, show the operation of the FQA and its output during 110° pitch rotations. During this experiment, α was set to 45°, and ϵ was 0.2. The bottom two subplots of Fig. 7 trace the value of $\cos\theta$ and the value of the switch flag that triggers the singularity avoidance method and show the direct correspondence between the two in time. It can be observed that, each time $\cos\theta$ was about to become less than ϵ, the switch flag was set to one. The top three subplots in Fig. 7 show the angles calculated from the quaternion estimate produced by the algorithm. The apparent rise of the pitch angle to 90° and then drop to 70° is a visualization artifact due to the use of the three angles for plotting purposes. A 110° pitch

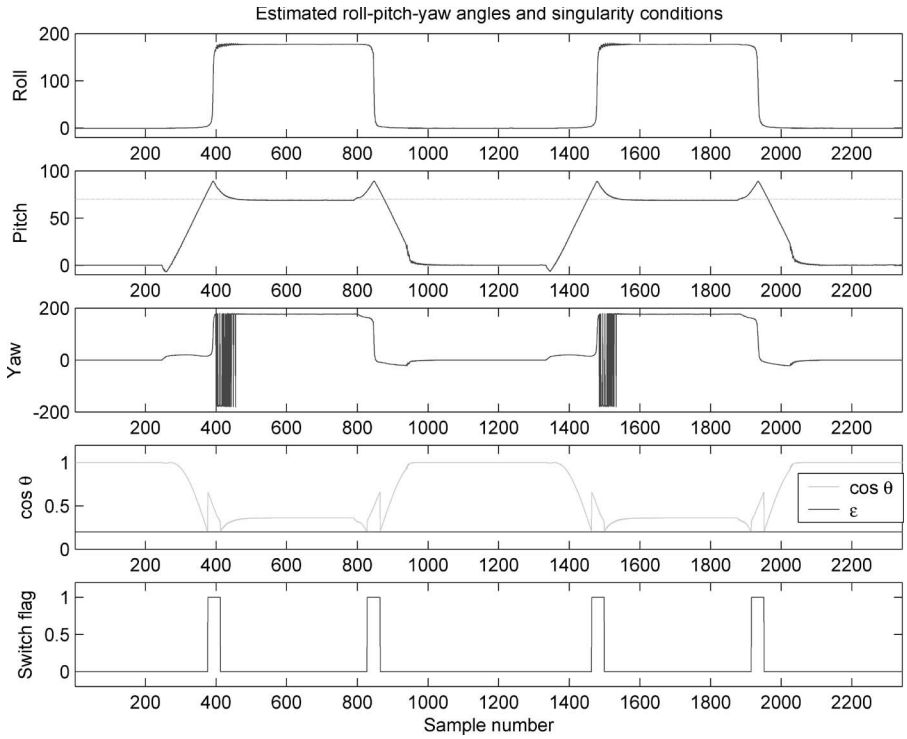

Fig. 7. Angles, singularity condition, and switch flag of the FQA during 110° rotation in pitch axis.

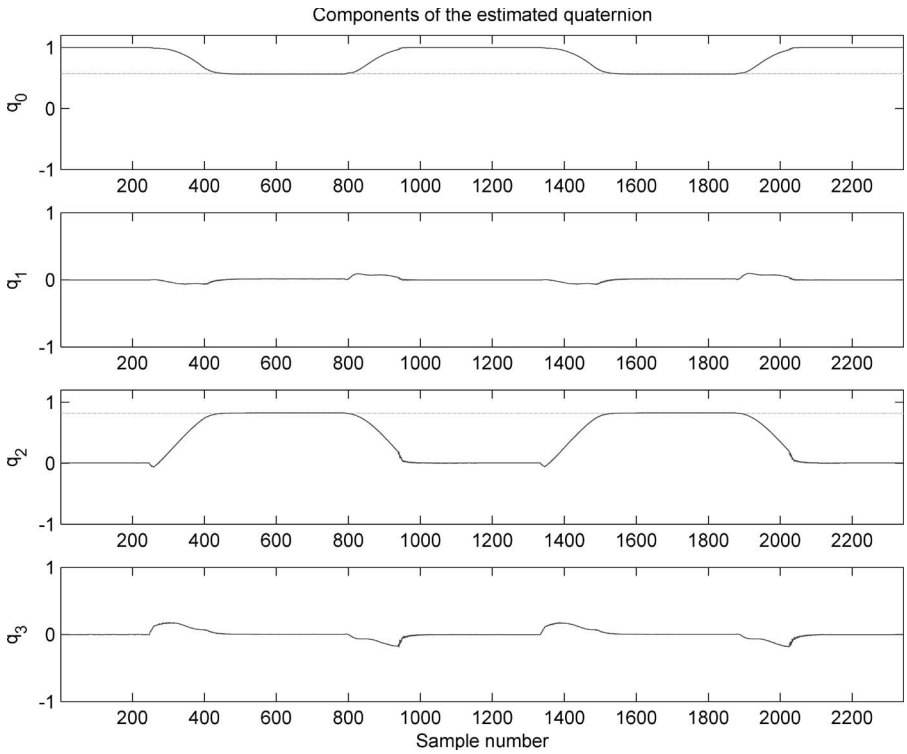

Fig. 8. Components of the estimated quaternion produced by the FQA during 110° rotation in pitch axis.

is represented as 70° pitch, together with a 180° roll and a $\pm 180°$ yaw. At times, the yaw angle flips between two alternate representations of the same rotation, namely, $-180°$ and 180°. The roll angle is stable at either 0° or 180°.

The quaternion elements that are shown in Fig. 8 are smooth and exhibit no flipping of orientation representations or singularity artifacts. The real part of the quaternion q_0 begins at 1.0 and changes to $\cos(110°/2) = 0.5736$ during the 110° rotations. The element of the unit quaternion associated with rotations about the pitch axis q_2 begins at zero and changes to $\sin(110°/2) = 0.8192$ during the 110° rotations. The small changes in q_1 and q_3 are due to misalignment

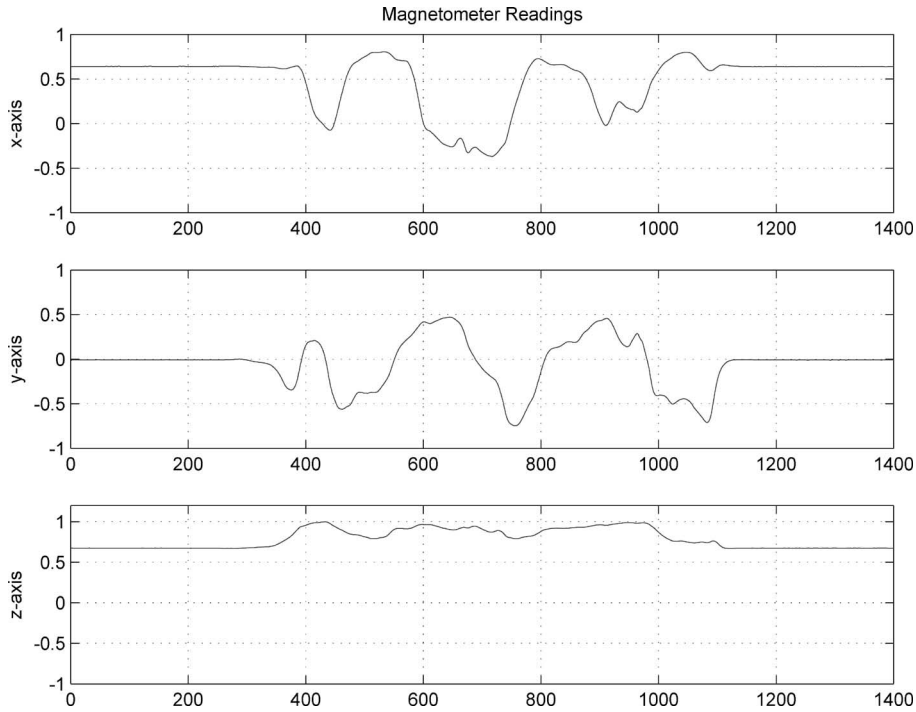

Fig. 9. Components of the normalized local magnetic field measurement vector under the influence of a moving magnetic field distortion.

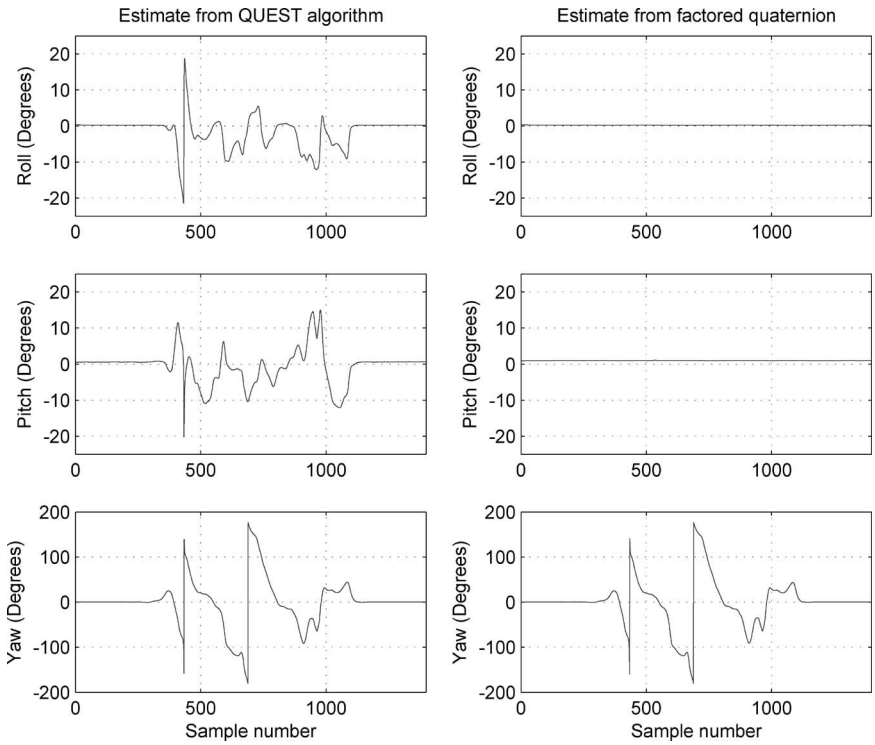

Fig. 10. Orientation estimate produced by the QUEST algorithm and FQA with a static sensor module under the influence of a moving magnetic field distortion.

between the sensor module and the motion axes of the tilt table.

C. Testing of Static Accuracy When Subjected to Magnetic Field Variations

To test the decoupling property of the FQA, an inertial/magnetic sensor module was mounted on a level nonferrous stationary platform. The sensor module $x_s y_s z_s$-axes were, respectively, aligned with the NED directions. Following an initialization period, the sensor module was exposed to a ferrous object. Movement of the ferrous object caused the direction of the measured magnetic field to rotate by as much as 360°. Changes in the measured magnetic field were observed in all measurement axes, as shown in Fig. 9. Fig. 10 shows orientations calculated using the QUEST algorithm and

FQA. It can be observed that the orientations calculated using the QUEST algorithm (depicted by three subplots to the left) exhibited errors on all axes. On the other hand, the FQA (depicted by three subplots to the right) showed no errors in either the pitch or roll axes.

D. Algorithm Efficiency

To make a rough comparison of the efficiency of the QUEST algorithm and FQA, the time required for each to complete the computation of 5000 orientation quaternions was determined using MATLAB on a PC with an 866-MHz Pentium III processor and 256-MB RAM. This number represents 50 s of data at a sampling rate of 100 Hz. Both algorithms were able to complete the 5000 quaternion calculations in less than 10 s. The calculations were completed in 9.8 s by the QUEST algorithm and 7.8 s by the FQA. In this experiment, the FQA was approximately 25% faster than the QUEST algorithm.

IV. Conclusion

This paper presents a physically intuitive algorithm for calculating orientation using accelerometer and magnetometer data for static or slow-moving objects. The algorithm produces estimates in quaternion form through a series of sequential rotations. These rotations can individually be examined in a manner similar to pitch, roll, and yaw angles in a Euler angle sequence. However, unlike Euler angles, the algorithm incorporates a singularity avoidance method. In the algorithm, magnetometer data are not used to calculate orientation that is relative to the vertical axis; thus, magnetic variations result in errors only in the horizontal plane. This property of the algorithm is experimentally demonstrated. Singularities in the numerical implementation are avoided through the use of a method that assigns an offset body coordinate system when a singularity occurs. The algorithm is efficient and does not require the evaluation of trigonometric functions. Experimental results indicate that, when combined with a low-pass filter for accelerometer data, the algorithm is able to track orientation. The algorithm has been successfully used in real-time human-body-motion-tracking applications.

As a final remark, it should be noted that dynamic estimation of an orientation quaternion through integration of values for $\dot{q}$ that are obtained from angular rate sensors is equally likely to produce a quaternion with a negative real part as a positive real part. On the other hand, the FQA always produces a quaternion with a positive real part. Since both q and $-q$ produce identical rotations, it is important to use both of these values in computing Δq, which is the difference between the predicted and measured value for q that is used in drift correction, and to then choose the value for Δq which is smaller in absolute value. This comparison is not necessary in some previous (less efficient and less accurate) approaches to drift correction [21] since these methods usually directly incorporate old estimates of q into estimation of Δq, while this is not the case for the FQA estimate.

Acknowledgment

The authors would like to thank J. Calusdian for his technical support during the course of this project, A. Kavousanos-Kavousanakis for implementing the QUEST algorithm, and C. Aparicio for implementing the FQA.

References

[1] E. Foxlin, M. Harrington, and Y. Alshuler, "Miniature 6DOF inertial for track HMDs," in *Proc. SPIE—Helmet Head-Mounted Displays III, AeroSense*, Orlando, FL, Apr. 1998, vol. 3362, pp. 214–228.

[2] E. Foxlin, "Inertial head-tracker fusion by a complementary separate-bias Kalman filter," in *Proc. VRAIS*, Santa Clara, CA, Mar. 1996, pp. 185–194.

[3] E. R. Bachmann, "Inertial and magnetic tracking of limb segment orientation for inserting humans into synthetic environments," Ph.D. dissertation, Naval Postgraduate School, Monterey, CA, 2000.

[4] E. R. Bachmann, R. B. McGhee, X. Yun, and M. J. Zyda, "Inertial and magnetic posture tracking for inserting humans into networked virtual environments," in *Proc. ACM Symp. VRST*, Banff, AB, Canada, Nov. 2001, pp. 9–16.

[5] A. Gallagher, Y. Matsuoka, and W.-T. Ang, "An efficient real-time human posture tracking algorithm using low-cost inertial and magnetic sensors," in *Proc. IEEE Int. Conf. Robot. Autom.*, Sendai, Japan, Sep. 28–Oct. 2, 2004, pp. 2967–2972.

[6] H. J. Luinge, "Inertial sensing of human movement," Ph.D. dissertation, Univ. Twente, Enschede, The Netherlands, Dec. 2002.

[7] R. Zhu and Z. Zhou, "A real-time articulated human motion tracking using tri-axis inertial/magnetic sensors package," *IEEE Trans. Neural Syst. Rehabil. Eng.*, vol. 12, no. 2, pp. 295–302, Jun. 2004.

[8] Z. Yan and K. Yuan, "An orientation tracking algorithm valid in a hemisphere space based on gravity field and Earth magnetic field," in *Proc. IEEE Int. Conf. Inf. Acquistion*, Hefei, China, Jun. 2004, pp. 236–239.

[9] D. Gebre-Egziabher, G. H. Klkaim, J. Powell, and B. W. Parkinson, "A gyro-free quaternion-based attitude determination system suitable for implementation using low cost sensors," in *Proc. IEEE Position Location Navigation Symp.*, San Diego, CA, Mar. 2000, pp. 185–192.

[10] G. Wahba, "Problem 65-1: A least squares estimate of satellite attitude," *SIAM Rev.*, vol. 7, no. 3, p. 409, Jul. 1965.

[11] M. Shuster and S. Oh, "Three-axis attitude determination from vector observations," *J. Guid. Control*, vol. 4, no. 1, pp. 70–77, Jan./Feb. 1981.

[12] J. Farrell and J. Stuelpnagel, "A least squares estimate of spacecraft attitude," *SIAM Rev.*, vol. 8, no. 3, pp. 384–386, 1966.

[13] P. Davenport, "Attitude determination and sensor alignment via weighted least squares affine transformations," Goddard Space Flight Center, Greenbelt, MD, NASA X-514-71-312, 1965.

[14] M. D. Shuster and S. D. Oh, "Three-axis attitude determination from vector observations," *J. Guid. Control*, vol. 4, no. 1, pp. 70–77, Jan./Feb. 1981.

[15] R. B. McGhee, "The factored quaternion algorithm for orientation estimation from measured Earth gravity and magnetic field," MOVES Inst., Naval Postgraduate School, Monterey, CA, 2004, Tech. Memo. [Online]. Available: http://www.users.muohio.edu/bachmaer/Papers/Factored%20 Quaternion.pdf

[16] E. R. Bachmann, X. Yun, D. McKinney, R. B. McGhee, and M. J. Zyda, "Design and implementation of MARG sensors for 3-DOF orientation measurement of rigid bodies," in *Proc. IEEE Int. Conf. Robot. Autom.*, Taipei, Taiwan, R.O.C., May 2003, vol. 1, pp. 1171–1178.

[17] H. Goldstein, C. Poole, and J. Safko, *Classical Mechanics*, 3rd ed. Reading, MA: Addison-Wesley, 2002.

[18] J. B. Kuipers, *Quaternions and Rotation Sequences*. Princeton, NJ: Princeton Univ. Press, 1999.

[19] J. Stuelpnagel, "On the parameterization of the three-dimensional rotation group," *SIAM Rev.*, vol. 6, no. 4, pp. 422–430, Oct. 1964.

[20] M. D. Shuster and G. A. Natanson, "Quaternion computation from a geometric point of view," *J. Astronaut. Sci.*, vol. 41, no. 4, pp. 545–556, 1993.

[21] E. R. Bachmann and X. Yun, "A single parameter tunable quaternion based attitude estimation filer," *J. Inst. Navig.*, vol. 53, no. 2, pp. 109–120, 2006.

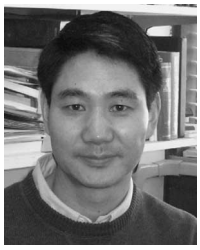

Xiaoping Yun (S'86–M'87–SM'96–F'05) received the B.S. degree from Northeastern University, Shenyang, China, in 1982 and the M.S. and D.Sc. degrees from Washington University, St. Louis, MO, in 1984 and 1987, respectively.

He is currently a Professor of electrical and computer engineering with the Naval Postgraduate School, Monterey, CA. His research interests include coordinated control of multiple robotic manipulators, mobile manipulators, mobile robots, control of nonholonomic systems, MEMS sensors, carbon-nanotube-based sensors, and human-body-motion tracking using inertial/magnetic sensors.

Dr. Yun was an Associate Editor of the IEEE TRANSACTIONS ON ROBOTICS AND AUTOMATION from 1993 to 1996 and a coeditor of the Special Issue on "Mobile Robots" of the *IEEE Robotics and Automation Society (RAS) Magazine* in 1995. He was the Cochair of the RAS Technical Committee on Mobile Robots during 1992–2003; a member of the RAS Conference Board during 1999–2003; a member of the Program Committee of IEEE International Conference on Robotics and Automation in 1990, 1991, 1997, 1999, 2000, 2003, and 2004; a member of the Program Committee of the IEEE/RSJ International Conference on Intelligent Robots and Systems in 1998, 2001, 2003, and 2004; the General Cochair of the 1999 IEEE International Symposium on Computational Intelligence in Robotics and Automation; the Finance Chair of the IEEE International Conference on Robotics and Automation in 2002 and 2004; the Finance Chair of the IEEE/RSJ International Conference on Intelligent Robots and Systems in 2001, 2004, 2005, and 2006; and the Finance Chair of the IEEE International Conference on Nanotechnology in 2001. He is the Treasurer of the IEEE Robotics and Automation Society for 2004–2007 and was the Vice President for Finance of the IEEE Nanotechnology Council during 2004–2006.

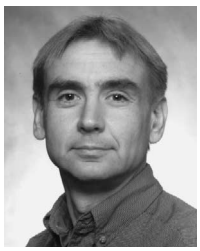

Eric R. Bachmann (M'01) received the Bachelor's degree from the University of Cincinnati, Cincinnati, OH, and the M.S. and Ph.D. degrees from the Naval Postgraduate School, Monterey, CA.

He is currently an Associate Professor with Miami University, Oxford, OH, and a Research Assistant Professor with the Naval Postgraduate School. Prior to this, he was an officer and an unrestricted naval aviator in the U.S. Navy. His research interests include virtual environments and posture and position tracking.

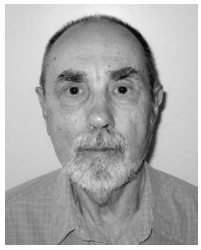

Robert B. McGhee (M'58–SM'85–F'90–LF'94) was born in Detroit, MI, in 1929. He received the B.S. degree in engineering physics from the University of Michigan, Ann Arbor, in 1952 and the M.S. and Ph.D. degrees in electrical engineering from the University of Southern California, Los Angeles, in 1957 and 1963, respectively.

From 1952 to 1955, he served on active duty as Guided Missile Maintenance Officer with the U.S. Army Ordnance Corps. From 1955 to 1963, he was a member of the Technical Staff with Hughes Aircraft Company, Culver City, CA, where he worked on guided missile simulation and control problems. In 1963, he joined the Department of Electrical Engineering, University of Southern California, as an Assistant Professor. He was promoted to Associate Professor in 1967. In 1968, he was appointed Professor of electrical engineering and Director of the Digital Systems Laboratory, The Ohio State University, Columbus. In 1986, he joined the Computer Science Department, Naval Postgraduate School, Monterey, CA, where he served as Department Chair from 1988 to 1992. Subsequently, he held the position of Professor of Computer Science until his retirement in 2004. He currently serves as Emeritus Professor and continues his involvement in ongoing research on human-motion tracking and related topics.